

# Simplification of High Frame Rate Imaging System with Coordinate Rotation

Jian-yu Lu and Sung-Jae Kwon, Department of Bioengineering, The University of Toledo, Toledo, OH 43606, USA. Email: jilu@eng.utoledo.edu

**Abstract** – A method to greatly simplify the high-frame-rate (HFR) imaging system using a rotation of coordinates in image reconstruction was developed. A theory of Fourier image reconstruction was also developed and both *in vitro* (on an AT539 tissue-mimicking phantom) and *in vivo* (on a human heart) experiments were performed to verify the theory.

**Keywords** - limited diffraction beams; high frame rate; HFR; medical imaging; beamforming

## I. INTRODUCTION

Based on the limited-diffraction beam theory [1]-[4], a high-frame-rate (HFR) imaging method for two-dimensional (2D) and three-dimensional (3D) imaging was developed in 1997 [5]-[9] and has been extended recently to explicitly include limited-diffraction array beam and steered plane wave transmissions to increase image field of view and to achieve equivalent dynamic focusing in both transmission and reception [10]-[19]. This method has the advantage that it could be implemented with simpler hardware than the conventional delay-and-sum (D&S) method [20] because the limited-diffraction array beam transmissions [21]-[23] can be approximated with square-wave aperture weightings [10] and the fast Fourier transform (FFT) can be used to reconstruct images. The method can also use multiple steered plane waves [5], [24]-[25].

In this paper, the HFR imaging method is further simplified using rotated Cartesian coordinates in which one of the rotated axes coincides with the transmission wave vector that corresponds to the central frequency of a 2D array transducer. A new mathematical relationship between the Fourier transform of a 3D object function and the limited-diffraction array beam weightings or 2D Fourier transform over the transducer aperture is developed. Images are reconstructed for various transmission wave vectors, rotated back, and then summed coherently (to obtain a high resolution, contrast, and large field of view) in the original coordinates to form the final image at a high frame rate. The summation could also be done incoherently to reduce speckles. With this method, the unnecessary high spatial-frequency components, which are produced by the off-axis transmit wave vectors, of the echo signals over the transducer aperture are greatly reduced. This allows the use of a larger sampling interval in the Fourier space, reducing the number of points in the fast Fourier transform (FFT) and the memory usage. In addition, a depth-dependent spatial filter can be more easily applied to increase signal-to-noise ratio by matching the filter bandwidth with the transverse spatial bandwidth of echo signals over depths (i.e., smaller spatial bandwidth at larger depths).

To verify the method, a home-made general-purpose high-frame rate imaging system [10], [26]-[27] was used to acquire radiofrequency (RF) echo signals from an AT539 tissue-mimicking phantom (ATS Laboratory, Inc) and a human heart. In the experiments, a 2.5-MHz center frequency, 128-element, and 19.2-mm aperture broadband phased-array transducer was used to obtain 2D images over a +/-45-degree field of view. The echo signals were digitized to 12 bits at 40 MHz. Results show that the method can greatly reduce the number of points required in the FFT operations while maintaining the quality of the reconstructed images.

## II. THEORY

The details of the theory of the HFR imaging method are given in [10] and thus will not be repeated here. With the X-wave formulas [1]-[4], one obtains a relationship between the Fourier transform of an object function and the RF echo signals as follows [10]:

$$\begin{aligned} \tilde{R}_{k_{x_R}+k_{x_T}, k_{y_R}+k_{y_T}}(\omega) &= \frac{A(k)T(k)H(k)}{c^2} \int_V f(\vec{r}_0) e^{i(\vec{k}^R + \vec{k}^T) \cdot \vec{r}_0} d\vec{r}_0 \\ &= \frac{A(k)T(k)H(k)}{c^2} F(\vec{K}^R + \vec{K}^T) \\ &= \frac{A(k)T(k)H(k)}{c^2} F'[(\vec{K}^R + \vec{K}^T)\Theta] \\ &= \frac{A(k)T(k)H(k)}{c^2} F'(k_{x_{R_2}}, k_{y_{R_2}}, k_{z_{R_2}} + k), \end{aligned} \quad (1)$$

where  $\tilde{R}_{k_{x_R}+k_{x_T}, k_{y_R}+k_{y_T}}(\omega)$  is the Fourier transform of the time-varying RF echo signal when the transducer receive aperture is weighted at the spatial frequencies  $k_{x_R}$  and  $k_{y_R}$ ,  $\vec{r}_0 = [x_0, y_0, z_0]^t$  and  $\vec{r}_2 = [x_2, y_2, z_2]^t$  are the original and rotated coordinates, respectively (rotating angles are  $\zeta_T$  and  $\theta_T$  in Fig. 1), the superscript,  $t$ , means a transpose of a vector or matrix,  $H(\omega/c) = \{1, \omega \geq 0; 0, \omega < 0\}$  is the Heaviside step function [28],  $A(k)$  and  $T(k)$  are the transmit and receive transfer functions, respectively [29],  $k = \omega/c$  is the wave number, where  $\omega = 2\pi f$  is the angular frequency, and  $f$  is the temporal frequency,  $c$  is the speed of sound,  $f(\cdot)$  and  $F(\cdot)$  are a 3D object function and its Fourier transform, respectively,  $V$  is the volume of the object.  $F'(\cdot)$  is the Fourier transform of  $f(\cdot)$  at the rotated coordinates.

This work was supported in part by a grant, HL60301, from the National Institutes of Health of USA.

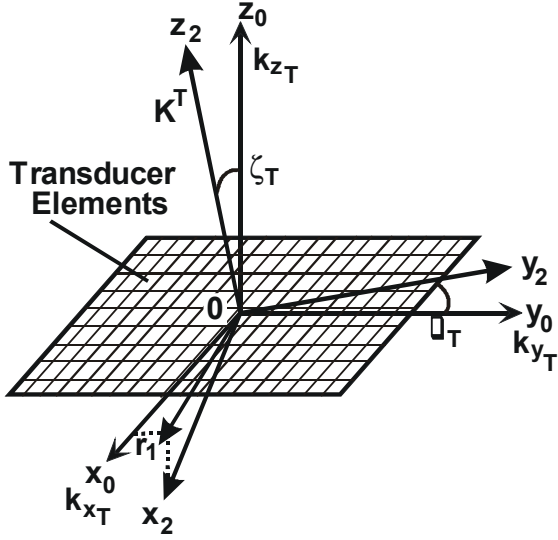


Figure 1. Coordinates before ( $\vec{r}_0$ ) and after rotation ( $\vec{r}_2$ ).

The transmission and reception wave vectors are given by:

$$\vec{K}^T = (k_{x_T}, k_{y_T}, k_{z_T}) \quad \text{and} \quad \vec{K}^R = (k_{x_R}, k_{y_R}, k_{z_R}) \quad ,$$

respectively, where  $k_{z_T} = \sqrt{k^2 - k_{x_T}^2 - k_{y_T}^2}$  and

$$k_{z_R} = \sqrt{k^2 - k_{x_R}^2 - k_{y_R}^2} \quad .$$

The rotation matrix and its inversion are given by:

$$\Theta = \begin{bmatrix} \cos \zeta_T \cos \theta_T & -\sin \theta_T & \sin \zeta_T \cos \theta_T \\ \cos \zeta_T \sin \theta_T & \cos \theta_T & \sin \zeta_T \sin \theta_T \\ -\sin \zeta_T & 0 & \cos \zeta_T \end{bmatrix} \quad (2)$$

and

$$\Theta^{-1} = \begin{bmatrix} \cos \zeta_T \cos \theta_T & \cos \zeta_T \sin \theta_T & -\sin \zeta_T \\ -\sin \theta_T & \cos \theta_T & 0 \\ \sin \zeta_T \cos \theta_T & \sin \zeta_T \sin \theta_T & \cos \zeta_T \end{bmatrix} = \Theta^t \quad , \quad (3)$$

respectively.

If a point in the coordinates before and after the rotation is

given by  $\vec{r}_0 = x_0 \vec{i}_0 + y_0 \vec{j}_0 + z_0 \vec{k}_0$  and

$\vec{r}_2 = x_2 \vec{i}_2 + y_2 \vec{j}_2 + z_2 \vec{k}_2$ , respectively, one has:  $\vec{r}_0 = \Theta \vec{r}_2$  and

$\vec{r}_2 = \Theta^{-1} \vec{r}_0$ . In addition, one obtains:

$$\vec{K}_2^T = (k_{x_{T_2}}, k_{y_{T_2}}, k_{z_{T_2}}) = \vec{K}^T \Theta = (0, 0, k) \quad \text{and}$$

$$\vec{K}_2^R = (k_{x_{R_2}}, k_{y_{R_2}}, k_{z_{R_2}}) = \vec{K}^R \Theta \quad \text{for the transmit and receive wave}$$

vectors in the rotated coordinates (assuming the transmit wave vector is aligned with a rotated axis), respectively, where

$$k_{z_{T_2}} = \sqrt{k^2 - k_{x_{T_2}}^2 - k_{y_{T_2}}^2} \quad \text{and} \quad k_{z_{R_2}} = \sqrt{k^2 - k_{x_{R_2}}^2 - k_{y_{R_2}}^2} \quad .$$

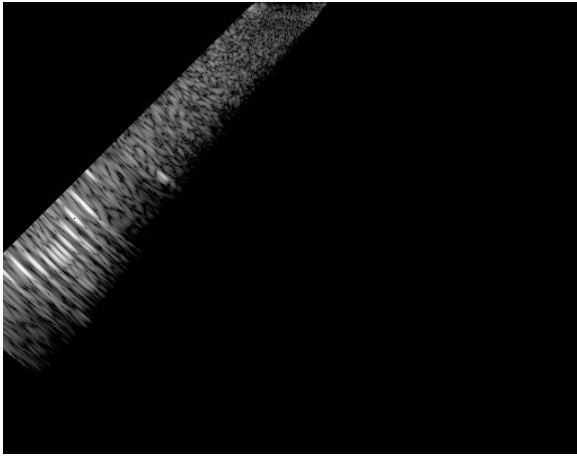
From the formulas above (Eq. (1)), it is clear that the relationship between the Fourier transform,  $F'(k_{x_{R_2}}, k_{y_{R_2}}, k_{z_{R_2}} + k)$ , of an object function,  $f(\vec{r}_0)$ , and the Fourier transform of received RF echo signals (can be easily rotated by linear phase delays) in the rotated coordinates is exactly the same as Equation (15) of [5], which is simpler to implement than that in the original coordinates.

### III. EXPERIMENTS AND RESULTS

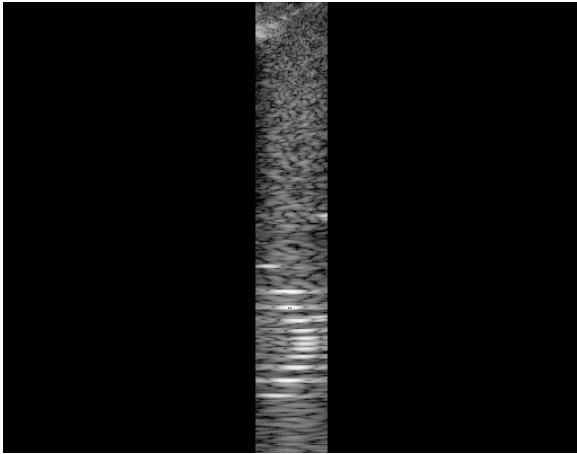
To verify the method and the formulas above, both *in vivo* and *in vitro* experiments were performed with a home-made HFR imaging system [10], [26]-[27]. The system has 128-channels to drive a 2.5-MHz broadband phase array transducer of 128 elements. RF echoes were digitized to 12 bits at 40 MHz and were used for image reconstructions.

Fig. 2 is a reconstructed strip of image of an ATS539 tissue-mimicking phantom with a single transmission steered at  $-45^\circ$ . After a rotation of the echo signals, the strip of image reconstructed with Eq. (1) is steered at  $0^\circ$  in the rotated coordinates (see Fig. 3). It is clear that the images reconstructed before and after the rotation are similar.

Figs. 4 and 5 are images reconstructed with and without the rotation of coordinates for an ATS539 tissue-mimicking phantom. Figs. 6 and 7 are images reconstructed with and without the rotation of coordinates for a human heart *in vivo*. The image frame rate is about 486 per second ( $187 \mu\text{s}$  between transmissions). The sizes of images in Figs. 2-7 are 153.6 mm in width and 120 mm in depth.



**Figure 2.** A strip of reconstructed image of an ATS539 tissue-mimicking phantom with one transmission steered at  $-45^\circ$  without coordinate rotation using Eq. (1) (see Reference [10] for details of image reconstructions).



**Figure 3.** A strip of reconstructed image of an ATS539 tissue-mimicking phantom with one transmission steered at  $-45^\circ$  with coordinate rotation using Eq. (1) (see Reference [10] for details of image reconstructions).

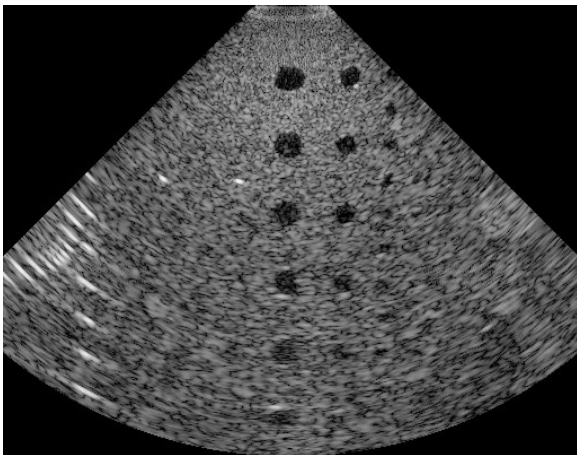


**Figure 4.** Reconstructed image of an ATS539 tissue-mimicking phantom with 11 transmissions steered from  $-45^\circ$  to  $45^\circ$  without coordinate rotation using Eq. (1) (see Reference [10] for details of image reconstructions).

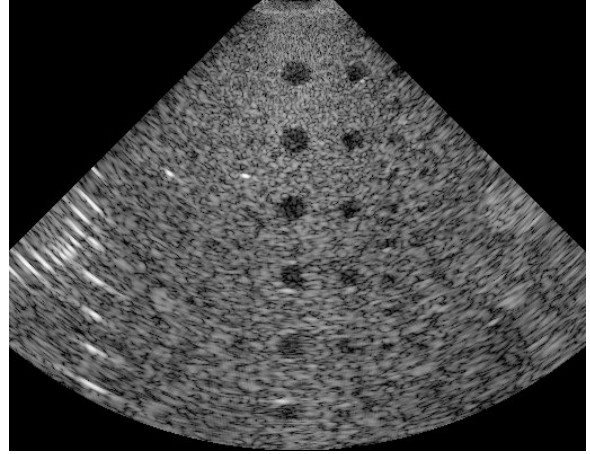


**Figure 5.** Reconstructed image of an ATS539 tissue-mimicking phantom with 11 transmissions steered from  $-45^\circ$  to  $45^\circ$  with coordinate rotation using Eq. (1) (see Reference [10] for details of image reconstructions).

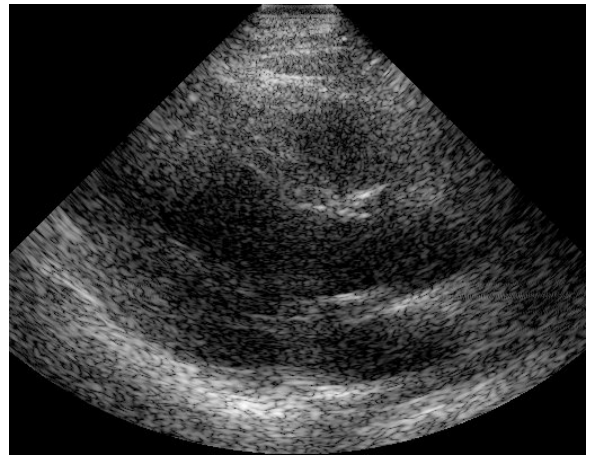


**Figure 6.** Reconstructed image of a human heart *in vivo* with 11 transmissions steered from  $-45^\circ$  to  $45^\circ$  without coordinate rotation using Eq. (1) (see Reference [10] for details of image reconstructions).

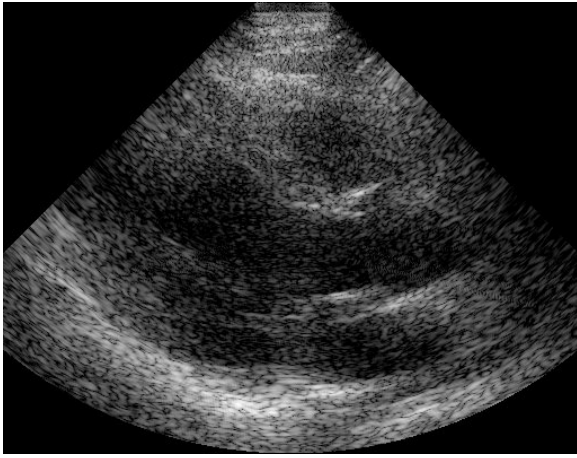


**Figure 7.** Reconstructed image of a human heart *in vivo* with 11 transmissions steered from  $-45^\circ$  to  $45^\circ$  with coordinate rotation using Eq. (1) (see Reference [10] for details of image reconstructions).

#### IV. CONCLUSION

The method developed using a rotation of coordinates may be useful to greatly reduce the complexity of imaging systems for reconstructing high-frame-rate images.

#### ACKNOWLEDGMENTS

This work was supported in part by a grant HL 60301 from the National Institutes of Health.

#### REFERENCES

- [1] Jian-yu Lu and J. F. Greenleaf, "Nondiffracting X waves --- exact solutions to free-space scalar wave equation and their finite aperture realizations," *IEEE Transactions on Ultrasonics, Ferroelectrics, and Frequency Control*, vol. 39, no. 1, pp. 19-31, January 1992.
- [2] Jian-yu Lu and J. F. Greenleaf, "Experimental verification of nondiffracting X waves," *IEEE Transactions on Ultrasonics, Ferroelectrics, and Frequency Control*, vol. 39, no. 3, pp. 441-446, May 1992.
- [3] Jian-yu Lu and Anjun Liu, "An X wave transform," *IEEE Transactions on Ultrasonics, Ferroelectrics, and Frequency Control*, vol. 47, no. 6, pp. 1472-1481, November 2000.
- [4] Charles Day, "Intense X-shaped pulses of light propagate without spreading in water and other dispersive media," *Physics Today*, v.57, n.10, pp.25-26, October 2004.
- [5] Jian-yu Lu, "2D and 3D high frame rate imaging with limited diffraction beams," *IEEE Transactions on Ultrasonics, Ferroelectrics, and Frequency Control*, vol. 44, no. 4, pp. 839-856, July 1997.
- [6] Jian-yu Lu, "Experimental study of high frame rate imaging with limited diffraction beams," *IEEE Transactions on Ultrasonics, Ferroelectrics, and Frequency Control*, vol. 45, no. 1, pp. 84-97, January 1998.
- [7] Jian-yu Lu, "Transmit-receive dynamic focusing with limited diffraction beams," in *1997 IEEE Ultrasonics Symposium Proceedings*, 97CH36118, vol. 2, pp. 1543-1546, 1997 (ISSN: 1051-0117).
- [8] Hu Peng and Jian-yu Lu, "High frame rate 2D and 3D imaging with a curved or cylindrical array," in *2002 IEEE Ultrasonics Symposium Proceedings*, 02CH37388, vol. 2, pp. 1725-1728, 2002 (ISSN: 1051-0117).
- [9] Glen Wade, "Human uses of ultrasound: ancient and modern," *Ultrasonics*, vol. 38, pp.1-5, 2000.
- [10] Jian-yu Lu, Jiqi Cheng, and Jing Wang, "High frame rate imaging system for limited diffraction array beam imaging with square-wave aperture weightings," *IEEE Transactions on Ultrasonics, Ferroelectrics, and Frequency Control*, vol. 53, no. 10, pp. 1796-1812, October 2006.
- [11] Jian-yu Lu and Jiqi Cheng, "System for extended high frame rate imaging with limited diffraction beams," *United States Patent* (Pending).
- [12] Jian-yu Lu, "High frame rate imaging system," *United States Patent* (Pending).
- [13] Jiqi Cheng and Jian-yu Lu, "Fourier based imaging method with steered plane waves and limited-diffraction array beams," in *2005 IEEE Ultrasonics Symposium Proceedings*, 05CH37716C, vol. 2, pp. 1976-1979, 2005 (ISSN: 1051-0117).
- [14] Jiqi Cheng and Jian-yu Lu, "Extended high frame rate imaging method with limited diffraction beams," *IEEE Transactions on Ultrasonics, Ferroelectrics, and Frequency Control*, vol. 53, no. 5, pp. 880-899, May 2006.
- [15] Jing Wang and Jian-yu Lu, "Effects of phase aberration and noise on extended high frame rate imaging," *Ultrasonic Imaging*, vol. 29, no. 2, pp. 105-121, April 2007.
- [16] Jing Wang and Jian-yu Lu, "Motion artifacts of extended high frame rate imaging," *IEEE Transactions on Ultrasonics, Ferroelectrics, and Frequency Control*, vol. 54, no. 7, pp. 1303-1315, July 2007.
- [17] Jing Wang and Jian-yu Lu, "A study of motion artifacts of Fourier-based image construction," in *2005 IEEE Ultrasonics Symposium Proceedings*, 05CH37716C, vol. 2, pp. 1439-1442, 2005 (ISSN: 1051-0117).
- [18] Jian-yu Lu and Jing Wang, "Square-wave aperture weightings for reception beam forming in high frame rate imaging," in *2006 IEEE Ultrasonics Symposium Proceedings*, 06CH37777, vol. 1, pp. 124-127, 2006 (ISSN: 1051-0117).
- [19] Jian-yu Lu, Zhaohui Wang, and Sung-Jae Kwon, "Blood flow velocity vector imaging with high frame rate imaging methods," in *2006 IEEE Ultrasonics Symposium Proceedings*, 06CH37777, vol. 2, pp. 963-966, 2006 (ISSN: 1051-0117).
- [20] Bernard D. Steinberg, "Digital beamforming in ultrasound," *IEEE Transactions on Ultrasonics, Ferroelectrics, and Frequency Control*, vol. 39, no. 6, pp. 716-721, November 1992.
- [21] Jian-yu Lu, "Limited diffraction array beams," *International Journal of Imaging System and Technology*, vol. 8, no. 1, pp. 126-136, January 1997 (ISSN: 0899-9457).
- [22] Jian-yu Lu, "Improving accuracy of transverse velocity measurement with a new limited diffraction beam," in *1996 IEEE Ultrasonics Symposium Proceedings*, 96CH35993, vol. 2, pp. 1255-1260, 1996 (ISSN: 1051-0117).
- [23] Jian-yu Lu and Jiqi Cheng, "Field computation for two-dimensional array transducers with limited diffraction array beams," *Ultrasonic Imaging*, vol. 27, no. 4, pp. 237-255, October 2005.
- [24] Jian-yu Lu and Shiping He, "Increasing field of view of high frame rate ultrasonic imaging," *Journal of Acoustical Society of America*, vol. 107, no. 5, pt. 2, pp. 2779, May 2000 (abstract).
- [25] Jian-yu Lu, "Nonlinear processing for high frame rate imaging," *Journal of Ultrasound in Medicine*, vol. 18, no. 3 (Supplement), p. S50, March 1999 (abstract).
- [26] Jian-yu Lu and John L. Waugaman, "Development of a linear power amplifier for high frame rate imaging system," in *IEEE 2004 Ultrasonics Symposium Proceedings*, 04CH37553C, vol. 2, pp. 1413-1416, 2004 (ISSN: 0-7803-8413-X).
- [27] Jian-yu Lu, "A multimedia example," *IEEE Transactions on Ultrasonics, Ferroelectrics, and Frequency Control*, vol. 50, no. 9, pp. 1078, September 2003.
- [28] R. Bracewell, *The Fourier Transform and its Applications*. New York: McGraw-Hill, 1965, Ch. 4 and 6.
- [29] Gordon S. Kino, *Acoustic Waves: Devices, Imaging and Analog Signal Processing*, Englewood Cliffs, N.J. : Prentice-Hall, 1987.